

UTILIZATION OF SPENT ANTHRACITE FILTER MEDIA IN CEMENT MORTAR: STRENGTH AND DURABILITY ASSESSMENT

*Phattharachai Pongsopha¹

¹Department of Civil Engineering, Rajamangala University of Technology Phra Nakhon, Thailand

*Corresponding Author, Received: 11 Sep. 2025, Revised: 22 Nov. 2025, Accepted: 03 Dec. 2025

ABSTRACT: This study investigates the utilization of spent anthracite filter media (SAFM) as a sustainable fine aggregate to partially replace natural sand in cement mortar. The experimental program evaluated the effects of SAFM replacement at 10%, 20%, and 30% by volume on the flowability, density, mechanical properties, and chemical durability under aggressive environments (NaCl, MgSO₄, and H₂SO₄). Mortar mixtures were prepared following ASTM standards with a constant water-to-cement ratio of 0.43. The results revealed that increasing SAFM content reduced the flow value from 115% (control) to 100% (30SAFM) and slightly decreased the density from 2136.0 to 2028.0 kg/m³ due to the lower specific gravity of SAFM. In contrast, the compressive and flexural strengths increased significantly by approximately 46% and 21%, respectively, at 30% replacement, indicating improved interfacial bonding and pore refinement. Durability tests demonstrated that SAFM enhanced resistance to chloride and sulfate attack, particularly under MgSO₄ exposure, where compressive strength after 90 days increased by 48% compared with the control. Although all specimens deteriorated under acidic conditions (H₂SO₄), SAFM delayed surface damage and mass loss. The findings confirm that SAFM can serve as an effective and eco-friendly alternative to natural sand, offering enhanced strength and durability while promoting the circular economy through waste reuse in sustainable construction materials.

Keywords: Spent anthracite filter media (SAFM), Mortar, Compressive strength, Durability, Sustainable construction

1. INTRODUCTION

The global construction industry heavily depends on natural river sand as the main fine aggregate in the production of mortar and concrete. However, increasing urbanization and infrastructure development have accelerated sand consumption to approximately 50 billion tons per year, making it the second most consumed natural resource after water [1]–[5]. Overextraction of sand has led to severe environmental degradation, including riverbank erosion, loss of aquatic habitats, and soil instability [5]–[7]. This crisis underscores the urgent need to identify and develop sustainable fine aggregate alternatives in alignment with the United Nations Sustainable Development Goals (SDGs 11 and 12).

Among the various waste materials investigated, spent anthracite filter media (SAFM) from water-treatment plants present a promising candidate due to their physical durability, angular morphology, and high carbon content [8]–[14]. During its use in filtration systems, anthracite gradually accumulates inorganic and organic contaminants, necessitating periodic replacement. As a result, large quantities of discarded SAFM are produced annually, creating significant disposal challenges and environmental concerns. In practical operation, the replacement of exhausted anthracite from water-treatment filters generates substantial solid waste. A standard dual-media filtration unit with a surface area of approximately 40 m² and an anthracite layer depth of

0.6 m produces around 24 m³ (\approx 19.7 t) of spent anthracite per replacement cycle. For a medium-sized municipal treatment plant equipped with six filters, this corresponds to roughly 118 t of SAFM per replacement, or 20–25 t annually based on a 5-year replacement interval. Given the extensive number of municipal and industrial filtration systems operating across Thailand, the total annual generation of SAFM waste is estimated to exceed several thousand tonnes, emphasizing the urgency of developing effective reuse strategies within the framework of sustainable and circular construction practices. [15]–[21] This waste stream is particularly critical in Asia, where the anthracite filter media market continues to expand rapidly [22]–[26]. Thus, recycling SAFM for construction applications could simultaneously address the issues of waste disposal and sand scarcity.

Previous studies on anthracite and other carbon-based by-products have yielded mixed results regarding workability and mechanical performance. For instance, Li et al. [27] observed that raw anthracite reduced the flowability of concrete due to its high porosity, whereas Singh and Siddique [36] reported strength enhancement in mortars containing coal bottom ash through improved interfacial bonding. Çelik et al. [28] demonstrated that waste glass fines increased chloride resistance by refining the pore network. Compared to these materials, SAFM exhibits both rough, angular surfaces (beneficial for mechanical interlocking) and a porous internal structure (which may enhance internal curing but

reduce flowability). Therefore, it is crucial to balance these competing effects to achieve optimal performance.

While numerous studies have examined anthracite and carbon-rich waste in cementitious materials, limited work has addressed the direct substitution of sand with spent anthracite filter media, particularly in terms of comprehensive mechanical and chemical durability evaluation. Moreover, no prior research has systematically correlated SAFM's physical properties (specific gravity, porosity, particle morphology) with its macro-scale effects on mortar performance under aggressive environments (NaCl, MgSO₄, and H₂SO₄).

This study bridges that gap by providing a comparative, data-driven evaluation of SAFM as a fine aggregate replacement in cement mortar. It investigates the influence of SAFM content (10-30% by volume) on flowability, density, compressive and flexural strengths, and long-term durability under different chemical exposures. The findings not only extend the understanding of anthracite-based aggregates but also establish new scientific insight into how SAFM's physical characteristics contribute to pore refinement, improved mechanical interlocking, and enhanced resistance to sulfate and chloride attacks. The research thus supports the circular economy by valorizing a previously underutilized industrial by-product for sustainable construction applications.

2. RESEARCH SIGNIFICANCE

This study introduces a sustainable approach to reusing spent anthracite filter media (SAFM), a by-product from water treatment plants, as a partial replacement for natural sand in cement mortar. The research addresses both the environmental issue of sand depletion and the disposal of industrial waste while evaluating the effects of SAFM on workability, density, strength, and durability under various exposure conditions. The findings demonstrate that incorporating 20–30% SAFM enhances mechanical and durability performance through physical interlocking and improved packing density, offering a practical and eco-efficient solution that aligns with circular economy principles and promotes sustainable construction practices.

3. MATERIALS AND METHODS

3.1 Materials

Hydraulic cement conforming to ASTM C1157 [29] was used as the primary binder.

Natural river sand with a fineness modulus of 2.6 and a specific gravity of 2.63 served as the reference fine aggregate, and its grading profile is presented in Figure 2 for comparison with SAFM.

Spent anthracite filter media (SAFM) was collected from a water filtration system after being discarded following its filtration cycle. To ensure cleanliness and minimize potential contamination, the SAFM underwent a step-cleaning procedure. The SAFM was washed with tap water and immersed in a 1 M NaOH solution for 2 hours to remove surface impurities and organic residues. Mild alkaline cleaning has been proven effective in eliminating contaminants from carbon-based filter media without altering their mineral or physical structure. [30]-[33]

After alkaline soaking, SAFM was washed multiple times with distilled water.

The cleaned SAFM was oven-dried at 105 ± 5 °C for 24 hours.

The dried media was then sieved to comply with the ASTM C33 [34] gradation for fine aggregates.

Its physical properties, including specific gravity, bulk density, and water absorption, were determined in accordance with ASTM C128 [35]. Tap water, meeting ASTM C1602 requirements [36], was used for mixing.



Fig.1 Spent anthracite filter media (SAFM)

Table 1. Properties of SAFM

Specification	Typical Value
Specific Gravity	1.6 g/cm ³
Bulk Density (dry)	820 kg/m ³
Water Absorption	2-3%

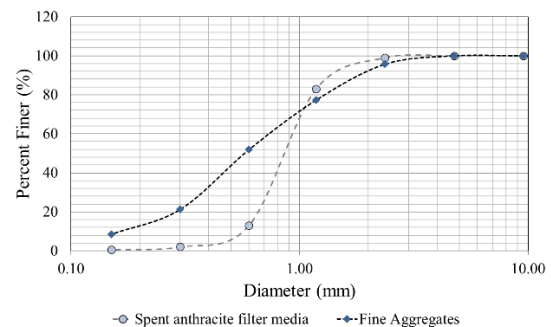


Fig.2 Particle size distribution

The particle size distribution of SAFM was determined using standard sieve fractions, and the resulting grading curve is presented in Figure 2. SAFM exhibited a broader distribution and a slightly finer fraction compared with natural sand, although both materials fall within the acceptable gradation range for fine aggregates. This ensures compatibility with mortar production requirements and allows SAFM to be used as a partial sand replacement without modifying the mix design framework.

3.2 Mix Proportions

Mortar mixtures were designed with a binder-to-sand ratio of 1:2.75 by mass, following ASTM C109 guidelines [37]. The water-to-cement ratio (w/c) was fixed at 0.43 for all mixtures. Natural sand was replaced with SAFM at 0%, 10%, 20%, and 30% by volume. Mix proportions are summarized in Table 2.

Table 2. Mix proportions

Name	Mix proportions (kg/m ³)			
	Cement (kg)	FA (kg)	SAFM (kg)	Water (kg)
Control	490	1348	-	210
10SAFM	490	1213	83	210
20SAFM	490	1070	166	210
30SAFM	490	943	249	210

Note: FA : Fine aggregate , SAFM : Spent anthracite filter media

3.3 Specimen Preparation

Mixing was performed using a laboratory mortar mixer in accordance with ASTM C305 [38]. Mortar cubes (50 × 50 × 50 mm) were prepared for compressive strength tests, while prisms (40 × 40 × 160 mm) were cast for flexural strength evaluation. For flowability testing, fresh mortar was tested using the flow table method as per ASTM C1437 [39]. After casting, specimens were covered with plastic sheets for 24 h and then demolded. All samples were cured in water at 27 ± 2 °C until the designated testing ages of 28 and 90 days.

3.4 Test Methods

• Flowability: Determined using the flow table test following ASTM C1437 [39].



Fig. 3 Flow Table Test

- Density: Measured according to ASTM C138 [40] by mass-to-volume ratio.
- Compressive Strength: Tested on 50 mm cubes at 28 and 90 days following ASTM C109 [37]



Fig. 4 Compression Test

- Flexural Strength: Conducted on 40 × 40 × 160 mm prisms using three-point bending per ASTM C348 [41].



Fig. 5 Flexural Test

3.5 Chemical Durability Tests

Durability assessment was conducted by immersing 28 day cured mortar specimens in aggressive solutions for up to 90 days

After 28 days of water curing, the specimens were immersed in aggressive chemical solutions for 90 days:

- 5% NaCl solution,
- 5% MgSO₄ solution, and
- 3% H₂SO₄ solution (by mass of water).

The testing procedure was conducted following the general guidelines of ASTM C1012/C1012M [42] for sulfate resistance, with necessary modifications for mortar cubes. The NaCl and H₂SO₄ exposure tests were performed as adapted procedures based on ASTM C267 [43] to evaluate chemical resistance. Each container maintained the target concentration, and solutions were refreshed every 14 days to ensure consistency. After exposure, the specimens were visually examined and tested for compressive

strength to assess deterioration and durability performance.

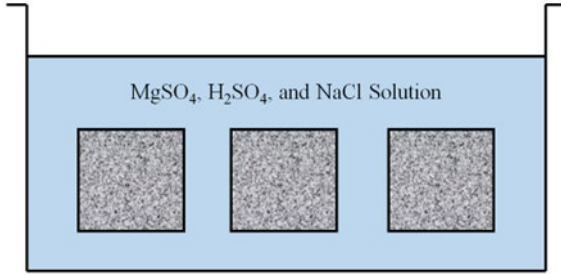


Fig.6 Mortar specimens immersed in MgSO₄, H₂SO₄, and NaCl solutions

4. RESULTS

This section presents the experimental results of mortar mixtures in which natural sand was partially replaced with spent anthracite filter media (SAFM) at replacement levels of 10%, 20%, and 30%, compared with a control mortar. The evaluation covers both fresh and hardened properties, including flowability, density, compressive strength, flexural strength, long-term compressive strength under different curing environments, and damage characteristics under aggressive solutions.

4.1 Flowability

The flowability of the mortar mixtures decreased with the increase of SAFM replacement. The control mortar exhibited a flow of 115%, while the 10%, 20%, and 30% SAFM mixtures demonstrated flow values of 108%, 104%, and 100%, respectively. As shown in Figure 7. This reduction is attributed to the rough texture and high water absorption capacity of SAFM particles, which hindered the free movement of cement paste around aggregates.

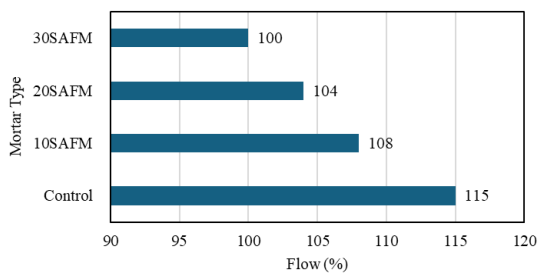


Fig.7 Flowability

The observed reduction in flowability (115% to 100%) aligns with previous findings by Li et al. and Rahman et al., who reported a 10–15% flow loss when using porous fine aggregates such as coal bottom ash or recycled glass. However, the SAFM

mixtures in this study exhibited relatively stable workability without additional water or admixture, showing better rheological stability compared with bottom-ash mortars [44]–[49].

4.2 Density

The density of mortars decreased slightly as the SAFM content increased, ranging from 2136 kg/m³ for the control to 2028 kg/m³ for the 30% SAFM mix. As shown in Figure 8. This is primarily due to the lower specific gravity of SAFM (1.60) compared to natural sand (2.63).

The observed 5% reduction in density is consistent with previous studies that utilized lightweight fine aggregates, such as expanded clay and recycled glass, which typically produce a 5–10% decrease [50]–[52]. This indicates that SAFM can achieve moderate weight reduction without compromising the overall strength performance of the mortar.

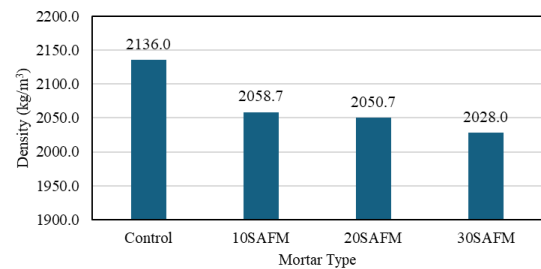


Fig.8 Density

4.3 Compressive Strength

The compressive strength increased as the SAFM content rose. The control mixture recorded 20.22 MPa, while the 10%, 20%, and 30% SAFM mixtures achieved 23.51, 26.74, and 29.60 MPa, respectively.

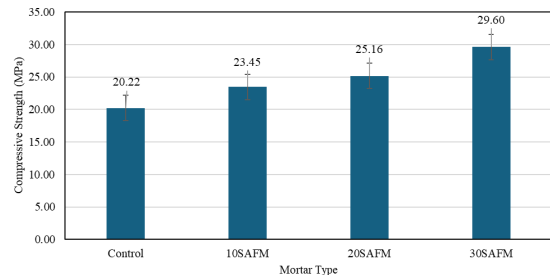


Fig.9 Compressive Strength

The increase in strength can be attributed mainly to physical and mechanical factors, including the angular and rough surface of SAFM particles, which improve mechanical interlocking between aggregate and paste. Additionally, SAFM's relatively lower stiffness compared to sand may help distribute stress more evenly within the mortar matrix.

In contrast to many porous or waste aggregates that reduce compressive strength by 5–20% [46], [47], the use of SAFM resulted in a remarkable 46% strength gain. Similar improvements in compressive strength have been reported for mortars incorporating angular fine aggregates such as crushed glass and ceramics [53],[54] confirming that particle geometry and interlocking behavior play a dominant role in load transfer and crack resistance rather than chemical effects.

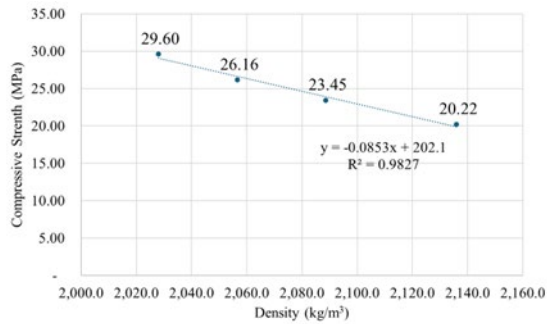


Fig.10 Relationship between density and compressive strength

The relationship between density and compressive strength of SAFM mortar mixtures exhibits a strong inverse correlation (Figure 10). As density decreases from 2136.0 kg/m³ (control) to 2028.0 kg/m³ (30% SAFM), the compressive strength increases from 20.22 MPa to 29.60 MPa, following the regression model $y = -0.0853x + 202.1$ with $R^2 = 0.9827$.

However, this statistical correlation should not be interpreted as a causal relationship. The decrease in density results primarily from the lower specific gravity of SAFM, whereas the strength enhancement is more plausibly influenced by physical–mechanical factors, including improved particle packing, the angularity of SAFM that promotes mechanical interlocking, and the modified water-demand behavior associated with its surface texture. These mechanisms help distribute stresses more efficiently and delay crack initiation despite the lower density.

Therefore, the inverse density–strength trend observed in this study is specific to SAFM mortar and should not be generalized as a universal rule for all lightweight or porous fine aggregates.

4.4 Flexural Strength

The flexural strength of the control mix was 1.19 MPa, which increased to 1.44 MPa (approximately 21% higher) for the 30% SAFM mixture. (Figure 11). This improvement is primarily associated with mechanical reinforcement effects, where the angular SAFM particles enhance stress transfer across the

matrix and help delay crack propagation under bending load.

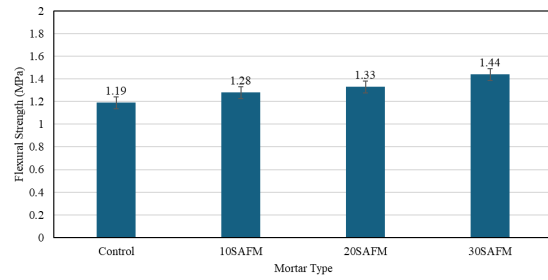


Fig.11 Flexural Strength

This 21% strength gain is greater than the <10% improvement typically observed in mortars containing recycled glass or ceramic sludge [55],[56],[57]. The enhanced performance suggests that SAFM’s shape and surface roughness promote better particle interlock and mechanical anchoring within the matrix, resulting in higher flexural capacity.

4.5 Compressive Strength at 90 Days under Different Curing Environments

The long-term compressive strength results at 90 days revealed clear differences depending on the exposure conditions (Figure 12). Underwater curing (90D-W), the control mortar achieved a strength of 23.7 MPa, whereas the SAFM mixtures exhibited higher values of 26.2, 29.7, and 32.3 MPa for 10%, 20%, and 30% replacement, respectively. This consistent increase indicates that SAFM contributes to better packing and stress transfer efficiency within the mortar matrix due to its angular shape and rough surface, which enhances mechanical interlocking between particles.

When exposed to NaCl solution (90D-NaCl), all mixtures recorded slightly higher strengths compared to water curing, with the maximum observed in the 30% SAFM mixture (34.1 MPa). The improvement can be attributed to the denser physical structure achieved by SAFM particles that reduce void spaces and restrict solution penetration. This trend agrees with previous studies using coal bottom ash and glass aggregates, where angular particles enhanced the overall compactness and reduced deterioration [53],[55].

In contrast, exposure to MgSO₄ solution (90D-MgSO₄) caused a reduction in compressive strength across all mixtures. The control dropped to 17.1 MPa, while SAFM mortars retained relatively higher values (20.3–25.3 MPa). The better performance of SAFM mortars is likely due to the tighter packing of fine particles, which physically slows down the ingress of

external solutions and minimizes internal stress concentration.

The most severe deterioration occurred under H_2SO_4 immersion (90D- H_2SO_4), where compressive strength declined sharply. The control mortar fell to 8.1 MPa, while SAFM mortars maintained slightly higher values (9.4–11.8 MPa). The reduced damage in SAFM mixtures can be attributed to their relatively denser and less permeable structure, which physically limits solution ingress and surface erosion. Although all specimens experienced degradation, SAFM mixtures displayed slower loss of integrity than the control, indicating improved mechanical cohesion between paste and aggregate.

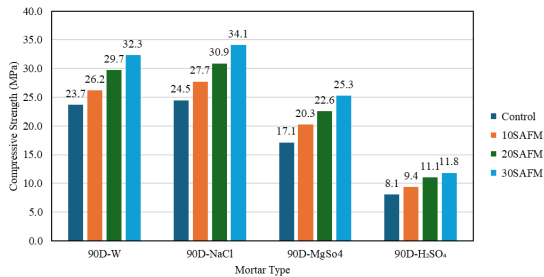


Fig.12 Compressive Strength at 90 Days under Different Curing Environments

4.6 Damage Characteristics under Different Environments

The visual inspections of mortar specimens after 90 days of exposure provided additional evidence consistent with the compressive strength results (Figure 13). Specimens cured in water (90D-W) remained intact and dense, with no visible surface deterioration in all mixtures, indicating that SAFM incorporation does not weaken the physical integrity of mortar under non-aggressive conditions. The consistent surface condition corresponds with the strength improvement trends observed in Figure 8, confirming that SAFM contributes to overall compactness and cohesion of the hardened matrix.

For specimens exposed to NaCl solution (90D-NaCl), neither control nor SAFM mortars showed significant surface scaling, spalling, or cracking. However, SAFM mixtures—particularly at 20% and 30% replacement—displayed smoother and more compact surfaces with fewer visible voids than the control. This suggests that the angular and rough SAFM particles enhance the mechanical interlock between components, which helps resist the surface pressure and minor stress induced by salt crystallization. Similar visual resistance to chloride-related surface damage was reported by Rahman et al. [53] in mortars with recycled glass, where the physical compactness of the mix contributed to reduced deterioration compared with natural-sand mortars. Under $MgSO_4$ exposure (90D- $MgSO_4$), all

specimens developed slight surface roughness and minor discoloration, but deterioration was more severe in the control mixture. SAFM mortars maintained comparatively uniform and stable surfaces. The improved appearance can be explained by the denser packing of SAFM particles, which physically reduces permeability and prevents localized stress concentration at the paste–aggregate interface.

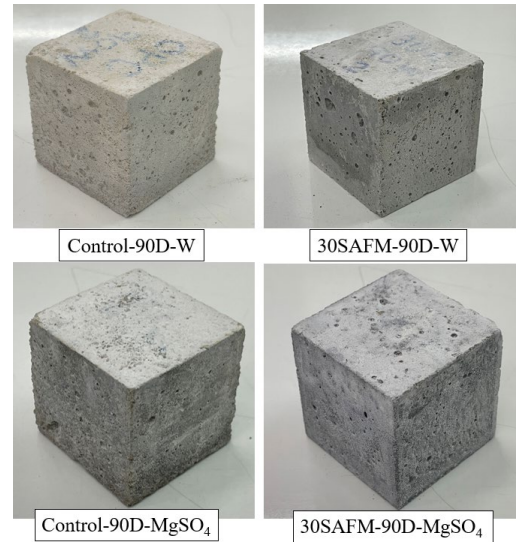


Fig.13a Surface appearance of control and 30 % SAFM mortars after 90 days of exposure to different environments.

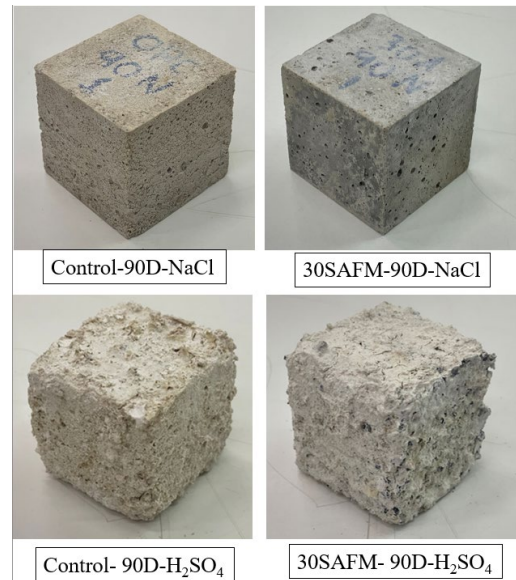


Fig.13b Surface appearance of control and 30 % SAFM mortars after 90 days of exposure to different environments.

In contrast, the specimens exposed to H_2SO_4 (90D- H_2SO_4) exhibited the most severe surface deterioration. All samples showed erosion and rounding of cube edges, particularly in the control and

10% SAFM mixtures, where surface material detached easily under slight pressure. The 20% and 30% SAFM mortars still displayed substantial damage but retained better physical cohesion, with less fragmentation and slower loss of corners. The enhanced surface integrity is likely due to the more compact structure formed by SAFM's angular particles, which physically limit acid penetration and slow the rate of surface erosion. Comparable findings have been noted in mortars containing dense ceramic fine aggregates, which showed improved resistance to disintegration through enhanced interparticle bonding.

Overall, the visual examination confirms that SAFM provides mechanical and physical improvement rather than chemical alteration. The mortars containing 20–30% SAFM exhibit visibly more cohesive and uniform surfaces under both chloride and sulfate exposure, supporting the quantitative strength data. However, all materials remain susceptible to severe damage under prolonged acid conditions, indicating that mechanical compactness alone is insufficient for extreme chemical environments.

5. DISCUSSION

The experimental results demonstrate that the incorporation of spent anthracite filter media (SAFM) as a partial replacement for natural sand significantly influences the fresh and hardened properties of cement mortar. Overall, SAFM enhances mechanical strength and durability while moderately reducing workability and density. These effects are primarily governed by the physical and mechanical characteristics of SAFM—particularly its angularity, surface roughness, and low specific gravity.

5.1 Workability and Density

The flow reduction observed with increasing SAFM content (from 115% to 100%) indicates higher internal friction and water absorption due to the irregular particle shape and rough surface of SAFM. Despite the reduction in flow, all mixes maintained workable consistency.

The density of mortar decreased slightly (approximately 5%) as SAFM replaced natural sand, attributed to SAFM's lower specific gravity (1.60 versus 2.63 for sand). Similar reductions have been reported in mortars containing lightweight fine aggregates. The decrease in unit weight may be advantageous for producing lightweight or non-structural mortars where reduced dead load is desirable.

5.2 Compressive and Flexural Strength

Contrary to many waste-based aggregates that often reduce strength due to weak particle–matrix

bonding, SAFM increased compressive strength by approximately 46% and flexural strength by 21% at 30% replacement. This improvement is primarily attributed to mechanical interlocking and enhanced stress distribution within the matrix, promoted by the angular geometry and rough texture of SAFM particles. These physical characteristics increase load transfer efficiency and crack resistance under compressive and flexural loading. Comparable improvements have been reported in mortars containing crushed glass and ceramic fines, where the particle morphology plays a critical role in enhancing mechanical properties.

5.3 Long-Term Strength and Durability

The 90-day compressive strength results under different curing environments confirmed the beneficial effects of SAFM. Under both water and NaCl curing, strength consistently increased with higher SAFM content, reaching 34.1 MPa at 30% replacement. The improved performance is attributed to the physically denser matrix created by the compact arrangement of SAFM particles, which reduces voids and limits the ingress of external solutions.

Under MgSO₄ exposure, all mortars exhibited some reduction in strength, but SAFM mixtures retained higher values (20.3–25.3 MPa) than the control (17.1 MPa). The enhanced stability is likely due to the compact aggregate skeleton, which minimizes expansion and cracking under sulfate pressure.

In the H₂SO₄ environment, all specimens deteriorated significantly; however, SAFM mortars maintained slightly higher residual strength (9.4–11.8 MPa) compared to the control. The improvement arises from the tighter particle packing and surface cohesion of SAFM mixtures, which physically slow the rate of surface erosion even under severe acidic attack.

5.4 Surface Integrity and Damage Behavior

Visual observations after 90 days support the mechanical findings. Under non-aggressive conditions, all specimens remained intact and dense. In NaCl and MgSO₄ exposure, SAFM mortars exhibited smoother and more uniform surfaces than the control, indicating better resistance to surface stress and physical degradation. Under H₂SO₄ immersion, although severe erosion occurred in all specimens, the 20% and 30% SAFM mortars displayed less fragmentation and better retention of shape.

The improved durability of the SAFM-mortars under NaCl and MgSO₄ exposure is likely driven by physical densification and reduced permeability rather than chemical alteration. The angular texture

and particle interlocking of SAFM minimize pore connectivity, thereby restricting ion transport and mitigating internal cracking. In $MgSO_4$ exposure, the denser matrix delays the formation of expansive products, resulting in less surface scaling and higher residual strength. However, under H_2SO_4 immersion, the marginal improvement indicates that the physical barrier effect of SAFM alone is insufficient to resist strong acid dissolution, emphasizing this limitation. These findings agree with recent observations that enhanced durability in modified mortars mainly originates from pore refinement and ion-diffusion control, while additional chemical stabilization is necessary for acid resistance. [57]

The optimal performance was achieved at 20–30% SAFM replacement, which provided the best balance between strength gain and manageable workability loss. From an engineering perspective, SAFM is suitable for applications requiring moderate strength and enhanced durability, such as masonry, plastering, and lightweight repair mortars. However, its performance in highly acidic conditions remains limited, suggesting that protective coatings or supplementary binders may be required for such environments.

Further research should examine the long-term dimensional stability, water absorption, and field performance of SAFM mortars under real exposure conditions. Investigations into thermal behavior, drying shrinkage, and acoustic performance may also broaden the potential applications of SAFM as a sustainable fine aggregate.

6. CONCLUSION

Based on the experimental findings, the following conclusions are drawn:

Flowability and Density: The incorporation of SAFM reduced flowability from 115% (control) to 100% (30SAFM) and decreased density from 2136.0 to 2028.0 kg/m^3 due to the lower specific gravity and rough, angular surface of SAFM particles.

Compressive Strength: Compressive strength improved from 20.22 MPa (control) to 29.60 MPa (30SAFM)—an increase of approximately 46%, attributed to enhanced interfacial bonding and microstructural densification.

Flexural Strength: Flexural strength increased by 21%, from 1.19 MPa (control) to 1.44 MPa (30SAFM), indicating better stress transfer and crack-bridging capacity.

Durability under Aggressive Environments (90 days):

- NaCl: Strength increased up to 34.1 MPa, showing improved chloride resistance.
- $MgSO_4$: SAFM mixtures retained 20.3–25.3 MPa, up to 48% higher than control (17.1 MPa).

- H_2SO_4 : All mixtures deteriorated, but 30SAFM retained higher residual strength (≈ 11.8 MPa) and reduced surface erosion.

Overall, the findings from this study demonstrate the technical feasibility and sustainability benefits of using spent anthracite filter media (SAFM) as a replacement for fine aggregate in cement mortar. By integrating waste reuse with performance enhancement, the findings contribute to reducing sand dependency and promoting circular construction practices. The established correlations between SAFM content and mechanical durability behavior provide a reference for practical implementation in eco-efficient mortars. Future research should expand on large-scale applications, evaluate long-term field performance, and explore synergy with supplementary cementitious materials to further optimize environmental and mechanical outcomes.

7. ACKNOWLEDGMENTS

The authors would like to sincerely acknowledge the support provided by “Rajamangala University of Technology Phra Nakhon (RMUTP)”. The facilities, technical assistance, and institutional resources made available by the university were indispensable to the successful execution of this research.

8. REFERENCES

1. Gallagher, L., and Peduzzi, P. (2019). Sand and sustainability: Finding new solutions for environmental governance of global sand resources. UNEP Report, 1–100. Retrieved from <https://archive-ouverte.unige.ch/unige:117767>
2. Sand, rarer than one thinks. (2014). Environmental Development, 11, 208–218. <https://doi.org/10.1016/j.envdev.2014.04.001>
3. Rentier, E. S., and Cammeraat, E. (2022). The environmental impacts of river sand mining. Science of the Total Environment, 838, 155877–155884. <https://doi.org/10.1016/j.scitotenv.2022.155877>
4. Bendixen, M., Best, J., Hackney, C., and Iversen, L. L. (2019). Time is running out for sand. Nature, 571(7763), 29–31. <https://doi.org/10.1038/d41586-019-02042-4>
5. Zavaleta, V. G., Nava, L. F., Kauffer, E., and Santana, O. G. (2023). Local knowledge of sediment exploitation in the Usumacinta River Basin: A theoretical–methodological framework proposal. Sustainability, 15(5), 4182–4195. <https://doi.org/10.3390/su15054182>
6. Sánchez, M. M., Parra, J. L., and Calvo, B. (2023). Exploration of natural aggregates for a sustainable construction industry in Western Colombia. Minerals, 13(11), 1430–1442. <https://doi.org/10.3390/min13111430>

7. Jordan, C., et al. (2019). Sand mining in the Mekong Delta revisited: Current scales of local sediment deficits. *Scientific Reports*, 9, 17879, 1–12. <https://doi.org/10.1038/s41598-019-53804-z>
8. da Silva, B. M. R., Bastos, R. K. X., and Bastos, P. K. X. (2021). Comparison of crushed rock sand and natural river sand as filter media for rapid filtration. *Water Science & Technology: Water Supply*, 21(1), 401–410. <https://doi.org/10.2166/ws.2020.311>
9. Ahmed, B. A., Ahmed, F., Ali, K., and Shabbir, J. (2020). Development and characterization of alumina-based membranes for water purification. *IOP Conference Series: Materials Science and Engineering*, 842, 012007, 1–7. <https://doi.org/10.1088/1757-899x/842/1/012007>
10. Kuchin, V. Yu., Detkova, T. V., Eliseev, A. A., and Reshiotkin, S. V. (2020). The study of the influence of the grain-size composition of anthracite on the agglomerating index. *IOP Conference Series: Materials Science and Engineering*, 718, 012009, 1–6. <https://doi.org/10.1088/1757-899x/718/1/012009>
11. Buiel, E., George, A. E., and Dahn, J. R. (1999). Model of micropore closure in hard carbon prepared from sucrose. *Carbon*, 37(9), 1399–1407. [https://doi.org/10.1016/S0008-6223\(98\)00335-2](https://doi.org/10.1016/S0008-6223(98)00335-2)
12. Davies, P. D. (2012). Alternative filter media in rapid gravity filtration of potable water. Ph.D. dissertation, Loughborough University, 1–200. Retrieved from <https://dspace.lboro.ac.uk/handle/2134/12183>
13. Tunggadewi, A. T., Hidiya, M., Sholihah, W., and Aziezah, N. (2023). Physical condition of filtrated wastewater from bakery household business. *E3S Web of Conferences*, 454, 02019, 1–5. <https://doi.org/10.1051/e3sconf/202345402019>
14. Wood, J. R., Storbråten, T., and Neubauer, T. (2020). Expansion and headloss dependencies for flowrate and fluidization during backwashing of sand, anthracite and Filtralite® filters. *Water*, 12(10), 2790–2801. <https://doi.org/10.3390/w12102790>
15. Westholm, L. J., Repo, E., and Sillanpää, M. (2014). Filter materials for metal removal from mine drainage: A review. *Environmental Science and Pollution Research*, 21(15), 9109–9128. <https://doi.org/10.1007/s11356-014-2903-y>
16. Tyulenev, M., Markov, S., Makridin, E., Lesin, Y., and Gogolin, V. A. (2019). Determination of the artificial filtering massif location for purification quarry wastewaters of Kamyshansky open pit mine. *E3S Web of Conferences*, 105, 02022, 1–7. <https://doi.org/10.1051/e3sconf/201910502022>
17. Zheng, Y. (2011). Mercury removal from cement plants by sorbent injection upstream of a pulse jet fabric filter. *Research Portal Denmark*, 1–279. Retrieved from <https://local.forskningportal.dk/local/dki-cgi/ws/cris-link?src=dtu&id=dtu-dd592443-2cb1-4c57-9c08-098a1773e329>
18. Wei, N. (2015). Leachability of heavy metals from lightweight aggregates made with sewage sludge and MSWI fly ash. *International Journal of Environmental Research and Public Health*, 12(5), 4992–5007. <https://doi.org/10.3390/ijerph120504992>
19. Chimenos, J. M., Fernández, A. I., Cervantes, A. B., Miralles, L., Fernández, M., and Espiell, F. (2005). Optimizing the APC residue washing process to minimize the release of chloride and heavy metals. *Waste Management*, 25(7), 686–693. <https://doi.org/10.1016/j.wasman.2004.12.014>
20. Masdiana, N., Rashid, M., Norruwaida, J., Hajar, S., Nabila, Z. H., and Ammar, M. R. (2020). Utilising formulated filter aids for toluene removal in filtration plant. *IOP Conference Series: Earth and Environmental Science*, 476, 012123, 1–6. <https://doi.org/10.1088/1755-1315/476/1/012123>
21. Wu, J., Cao, M., Tong, D., Finkelstein, Z., and Hoek, E. M. V. (2021). A critical review of point-of-use drinking water treatment in the United States. *npj Clean Water*, 4(1), 1–15. <https://doi.org/10.1038/s41545-021-00128-z>
22. Valliappan, V., and Sivapriya, S. V. (2024). Reuse of waste materials in geotechnical practice. *MATEC Web of Conferences*, 400, 02001, 1–5. <https://doi.org/10.1051/mateconf/202440002001>
23. Skoczko, I., and Gumiński, R. (2024). Tests on the application of various types of biomass for activated carbon production. *Journal of Ecological Engineering*, 25(1), 285–296. <https://doi.org/10.12911/22998993/174223>
24. Neamhom, T., Yakam, P., Bathbunrung, C., Tachavarong, W., Kosaisavee, V., and Pinatha, Y. (2025). Pilot-scale phosphorus recovery from mobile toilet wastewater in Bangkok, Thailand. *Scientific Reports*, 15, 87520, 1–12. <https://doi.org/10.1038/s41598-025-87520-8>
25. Visvanathan, C., and Cippe, A. (2001). Strategies for development of industrial wastewater reuse in Thailand. *Water Science & Technology*, 43(10), 59–66. <https://doi.org/10.2166/wst.2001.0580>
26. Kanchanapiya, P., and Tantisattayakul, T. (2022). Wastewater reclamation trends in Thailand. *Water Science & Technology*, 86(11), 2878–2887. <https://doi.org/10.2166/wst.2022.375>
27. Li, L., et al. (2017). A case of water absorption and water/fertilizer retention performance of super absorbent polymer modified sulphoaluminate cementitious materials. *Construction and Building Materials*, 150, 538–545. <https://doi.org/10.1016/j.conbuildmat.2017.05.219>

28. Çelik, A. İ., Kaya, S., and Baradan, B. (2022). Mechanical behavior of crushed waste glass as aggregate in concrete and mortars. *Materials*, 15(22), 8093, 1–12. <https://doi.org/10.3390/ma15228093>
29. ASTM C1157/C1157M-20. (2020). Standard performance specification for hydraulic cement. ASTM International, West Conshohocken, PA, 1–9.
30. Pachta, V., & Anastasiou, E. K. (2021). Utilization of Industrial Byproducts for Enhancing the Properties of Cement Mortars at Elevated Temperatures. *Sustainability*, 13(21), 12104. <https://doi.org/10.3390/su132112104>
31. Guo, H., et al. (2020). The effect of NaOH pretreatment on coal structure and biomethane production. *PLOS ONE*, 15(4), e0231623. <https://doi.org/10.1371/journal.pone.0231623>
32. Larasati, A., et al. (2020). Chemical regeneration of granular activated carbon: Preliminary evaluation of alternative regenerant solutions. *Environmental Science: Water Research & Technology*, 6(9), 2507–2516. <https://doi.org/10.1039/D0EW00328J>
33. Łązniewska-Piekarczyk, B., and Czop, M. J. (2025). Reclaimed municipal wastewater sand as a viable aggregate in cement mortars: Alkaline treatment and physical characterization. *Processes*, 13(8), 2463. <https://doi.org/10.3390/pr13082463>
34. ASTM C33/C33M. (2022). Standard specification for concrete aggregates. ASTM International, West Conshohocken, PA, 1–10.
35. ASTM C128. (2021). Standard test method for relative density (specific gravity) and absorption of fine aggregate. ASTM International, West Conshohocken, PA, 1–6.
36. ASTM C1602/C1602M. (2023). Standard specification for mixing water used in the production of hydraulic cement concrete. ASTM International, West Conshohocken, PA, 1–5.
37. ASTM C109/C109M. (2020). Standard test method for compressive strength of hydraulic cement mortars. ASTM International, West Conshohocken, PA, 1–9.
38. ASTM C305. (2021). Standard practice for mechanical mixing of hydraulic cement pastes and mortars. ASTM International, West Conshohocken, PA, 1–7.
39. ASTM C1437. (2020). Standard test method for flow of hydraulic cement mortar. ASTM International, West Conshohocken, PA, 1–6.
40. ASTM C138/C138M. (2022). Standard test method for density (unit weight), yield, and air content of concrete. ASTM International, West Conshohocken, PA, 1–7.
41. ASTM C348. (2020). Standard test method for flexural strength of hydraulic-cement mortars. ASTM International, West Conshohocken, PA, 1–6.
42. ASTM C1012/C1012M. (2023). Standard test method for length change of hydraulic-cement mortars exposed to a sulfate solution. ASTM International, West Conshohocken, PA, 1–11.
43. ASTM C267-01. (2012). Standard test method for chemical resistance of mortars, grouts, and monolithic surfacings. ASTM International, West Conshohocken, PA. <https://doi.org/10.1520/C0267-01R12>
44. Hamada, M. M., El-Gohary, S. M., Gomaa, A. M., and Kamel, M. M. (2022). Sustainable application of coal bottom ash as fine aggregates in concrete: A comprehensive review. *Case Studies in Construction Materials*, 16, e01109–e01125. <https://doi.org/10.1016/j.cscm.2022.e01109>
45. Burgmann, S., and Breit, A. (2024). Impact of crushed natural and recycled fine aggregates on fresh and hardened mortar properties. *Construction Materials*, 4(1), 37–57. <https://doi.org/10.3390/constrmater4010003>
46. Dong, W., Miller, S. A., and Xiao, L. (2023). Investigation of the performance of cement mortar incorporating lithium slag as a super-fine aggregate. *Frontiers in Materials*, 10, 1134622, 1–13. <https://doi.org/10.3389/fmats.2023.1134622>
47. Ullah, Shafi & Shahid, Muhammad & Tariq, Shadab & Khan, Ammad. (2021). Influence of Waste Marble Powder and Waste Granite Powder on the Mechanical and Durability Performance of Concrete. *Neutron*. 21. 46–51. <https://doi.org/10.29138/neutron.v21i1.134>
48. Chuang, C.-W., Chen, T.-A., and Huang, R. (2023). Effect of finely ground coal bottom ash as replacement for Portland cement on the properties of ordinary concrete. *Applied Sciences*, 13(24), 13212, 1–15. <https://doi.org/10.3390/app132413212>
49. Vălean, M., Manea, D. L., Aciu, C., Popa, F., Pleșa, L. M., Jumate, E., & Furtos, G. (2024). Performance Assessments of Plastering Mortars with Partial Replacement of Aggregates with Glass Waste. *Buildings*, 14(2), 507. <https://doi.org/10.3390/buildings14020507>
50. Cabrera-Covarrubias, F. G., Gómez-Soberón, J. M., Rosas-Casarez, C. A., Almaral-Sánchez, J. L., & Bernal-Camacho, J. M. (2021). Recycled Mortars with Ceramic Aggregates. Pore Network Transmutation and Its Relationship with Physical and Mechanical Properties. *Materials*, 14(6), 1543. <https://doi.org/10.3390/ma14061543>
51. Wan, X., Jia, Z., Li, N., and Luo, H. (2025). Impact of recycled fine aggregate on physical and mechanical properties of green mortar. *Materials*, 18(3), 696, 1–14. <https://doi.org/10.3390/ma18030696>
52. Zhao, Xiaoze & Xiaoli, Li & Xie, Weidong. (2024). Prediction of the rheological properties of mortar compounded with desert sand and Pisha sandstone ceramic sand based on density-form

- coupling. Scientific Reports, 14. <https://doi.org/10.1038/s41598-024-82240-x>
53. Çelik, A. İ., Özkılıç, Y. O., Zeybek, Ö., Karalar, M., Qaidi, S., Ahmad, J., Burduhos-Nergis, D. D., & Bejinariu, C. (2022). Mechanical Behavior of Crushed Waste Glass as Replacement of Aggregates. *Materials*, 15(22), 8093. <https://doi.org/10.3390/ma15228093>
54. Cabrera-Covarrubias, O., Mendoza-Rangel, J. M., López, R. R., and Martínez-Chavez, A. (2016). An experimental study of mortars with recycled ceramic aggregates. *Materials*, 9(12), 1029, 1–11. <https://doi.org/10.3390/ma9121029>
55. Rosado, S., Sánchez, A., Martínez, F. J., and Jiménez, E. A. (2022). Recycled aggregates from ceramic and concrete in mortar mixes: A study of their mechanical properties. *Materials*, 15(24), 8933, 1–14. <https://doi.org/10.3390/ma15248933>
56. Elemam, W. E., Agwa, I. S., and Tahwia, A. M. (2023). Reusing ceramic waste as a fine aggregate and supplemental cementitious material for sustainable concrete. *Buildings*, 13(11), 2726, 1–12. <https://doi.org/10.3390/buildings13112726>
57. Nuruddin, M., and Moghal, A. A. B. (2024). State-of-the-art review on the geotechnical and geoenvironmental feasibility of select biochars. *Indian Geotechnical Journal*, 54, 1073–1094. <https://doi.org/10.1007/s40098-023-00788-3>

Copyright © Int. J. of GEOMATE All rights reserved, including making copies, unless permission is obtained from the copyright proprietors.
